Published online 24 June 2021

Nucleic Acids Research, 2021, Vol. 49, No. 13 ***7347–7360***
https://doi.org/10.1093/nar/gkab536

Functional interplay of histone lysine 2-hydroxyisobutyrylation and acetylation in Arabidopsis under dark-induced starvation

Lanlan Zheng[1,2,†], Chen Li[1,2,†], Xueping Ma[1,2], Hanlin Zhou[3], Yuan Liu[3], Ping Wang[4], Huilan Yang[4], Yosuke Tamada[5], Ji Huang[6], Chunfei Wang[7], Zhubing Hu[7], Xuening Wang[8], Guodong Wang[8], Haihong Li[1], Juntao Hu[1], Xiaoyun Liu[4,*], Chao Zhou[3,*] and Yonghong Zhang[1,2,*]

[1]Hubei Key Laboratory of Embryonic Stem Cell Research, School of Basic Medicine, Taihe Hospital, Hubei University of Medicine, Shiyan 442000, China, [2]Hubei Key Laboratory of Wudang Local Chinese Medicine Research, Academy of Bio-Medicine Research, Hubei University of Medicine, Shiyan 442000, China, [3]Key Laboratory of Three Gorges Regional Plant Genetics & Germplasm Enhancement (CTGU) /Biotechnology Research Center, China Three Gorges University, Yichang 443002, China, [4]Institute for Interdisciplinary Research, Jianghan University, Wuhan 430056, China, [5]School of Engineering, Utsunomiya University, Utsunomiya 321-8585, Japan, [6]Center for Genomics and Systems Biology, Department of Biology, New York University, New York 10003, USA, [7]Center for Multi-Omics Research, Key Laboratory of Plant Stress Biology, State Key Laboratory of Cotton Biology, School of Life Science, Henan University, Kaifeng 475001, China and [8]College of Life Sciences, Shaanxi Normal University, Xi'an Shaanxi 710119, China

Received April 17, 2021; Revised June 02, 2021; Editorial Decision June 05, 2021; Accepted June 09, 2021

ABSTRACT

Lysine 2-hydroxyisobutyrylation (Khib) is a novel type of histone acylation whose prevalence and function in plants remain unclear. Here, we identified 41 Khib sites on histones in *Arabidopsis thaliana*, which did not overlap with frequently modified N-tail lysines (e.g. H3K4, H3K9 and H4K8). Chromatin immunoprecipitation-sequencing (ChIP-seq) assays revealed histone Khib in 35% of protein-coding genes. Most Khib peaks were located in genic regions, and they were highly enriched at the transcription start sites. Histone Khib is highly correlated with acetylation (ac), particularly H3K23ac, which it largely resembles in its genomic and genic distribution. Notably, co-enrichment of histone Khib and H3K23ac correlates with high gene expression levels. Metabolic profiling, transcriptome analyses, and ChIP-qPCR revealed that histone Khib and H3K23ac are co-enriched on genes involved in starch and sucrose metabolism, pentose and glucuronate interconversions, and phenylpropanoid biosynthesis, and help fine-tune plant response to dark-induced starvation. These findings suggest that Khib and H3K23ac may act in concert to promote high levels of gene transcription and regulate cellular metabolism to facilitate plant adaption to stress. Finally, HDA6 and HDA9 are involved in removing histone Khib. Our findings reveal Khib as a conserved yet unique plant histone mark acting with lysine acetylation in transcription-associated epigenomic processes.

INTRODUCTION

Chromatin is decorated with diverse epigenetic marks, such as DNA methylation and histone post-translational modifications (PTMs). These play crucial roles in regulating chromatin state and gene expression. One of the most prominent modifications, histone lysine acetylation (Kac), has long been recognized as an essential modification that regulates plant development and reversibly responds to environmental stress (1). More recent reports indicate that in addition to undergoing acetylation and methylation, lysine residues can be modified by diverse acylations by short-chain fatty acids, including propionylation, butyrylation (Kbu), crotonylation (Kcr), β-hydroxybutyrylation and 2-hydroxyisobutyrylation (Khib)

*To whom correspondence should be addressed. Tel: +86 719 8891147; Email: zhangyh@hbmu.edu.cn
Correspondence may also be addressed to Chao Zhou. Email: zhouchao@ctgu.edu.cn
Correspondence may also be addressed to Xiaoyun Liu. liuxiaoyun@jhun.edu.cn
†The authors wish it to be known that, in their opinion, the first two authors should be regarded as Joint First Authors.

(2–4). How these short-chain fatty acid acylations functionally interact with Kac has provoked broad interest. However, the role of histone acylation in plants has not been fully addressed.

Khib was initially identified as a widely distributed active histone mark in mammals (4). In yeast (*Saccharomyces cerevisiae*), the abundance of H4K8hib fluctuates in response to the availability of a carbon source, with low-glucose conditions leading to diminished Khib, implying that histone Khib is regulated by glucose homeostasis (5). In addition to histones, proteome-wide identifications have revealed that thousands of Khib modification sites exist on non-histone proteins in mammalian cells (6), moss (*Physcomitrium patens*) (7), and developing rice (*Oryza sativa*) seeds (8), implying that Khib is widely distributed across species and is involved in a wide range of molecular functions and cellular processes, including glycolysis/gluconeogenesis and tricarboxylic acid cycle. Although studies have suggested that H4K8hib interacts with histone Kac to coordinate diverse cellular processes by regulating gene transcriptional activities in yeast and mammals (4–6), whether the functional roles of histone Khib are conserved in plants, and how this histone mark interacts with the prevalent mark Kac and/or other modifications, have yet to be elucidated.

Histone PTMs are dynamically regulated by specific modifying enzymes whose activities require metabolites that serve as co-substrates or act as activators/inhibitors. Alternatively, cellular metabolism might influence histone modification in response to changing local concentrations of key metabolites (9). Acyl-Coenzyme A thioesters (Acyl-CoAs), which are intermediates in multiple, distinct metabolic pathways, serve as acyl donors in histone acylation, implying that histone acylation provides a link between cellular metabolism and epigenetic mechanisms (10). Histone short-chain acylations thus could link the metabolic state of the cell with chromatin architecture (2). Khib in mammals is thought to be derived from 2-hydroxyisobutyrate and 2-hydroxyisobutyryl-CoA (6). Given that the enrichment and recruitment of H4K8hib rely on an active glycolysis pathway in mammals (5) and that glycolysis is induced under both biotic and abiotic stress in plants (11), we were interested in exploring the role of histone Khib in the metabolic regulation of gene expression. Moreover, short-chain acyl-CoAs play vital roles in embryo development (12), although the entire process of fatty acid catabolism in *Arabidopsis thaliana* remains elusive (13). Therefore, identifying the functional roles of histone Khib in Arabidopsis could be crucial for unveiling the epigenetic mechanisms involved in primary metabolism in plant cells.

Fundamental breakthroughs in our understanding of the roles of histone PTMs have been made through the identification of the protein machineries that 'write' (incorporate), 'erase' (remove), and 'read' (bind) histone PTMs (14). The level of histone acetylation is reversibly determined by the actions of histone acetyltransferases (HATs) and deacetylases (HDACs) (15). Lysine butyrylation and propionylation can also be catalyzed and removed by HATs and deacetylases HDACs (3,16), suggesting that HATs and HDACs are involved in regulating histone acylation dynamics. Mammalian p300, a transcriptional coactivator that uses a number of different acyl-CoA cofactors, acts as a robust acetylase to catalyze multiple types of lysine acylations, such as propionylation and crotonylation (17). While p300 and the MYST family acetyltransferase Tip60 can catalyze Khib in mammalian cells, human HDAC2 (hHDAC2) and HDAC3 can both serve as Khib erasers (6,18). In plants, sirtuin histone deacetylase (SRT2) is involved in the removal of Kcr in rice (19). However, the enzymes that remove Khib modifications in Arabidopsis have not yet been characterized.

In the present study, we surveyed the genome-wide distribution patterns of histone Khib sites in Arabidopsis by mass spectrometry, and investigated the co-occurrence of Khib and Kac (in particular H3K23ac) via integrative comparative transcriptomic analysis. Both Khib and H3K23ac are associated with highly and ubiquitously expressed genes in various tissues, suggesting that Khib assists H3K23ac in promoting gene expression. To investigate whether and how histone Khib and H3K23ac affect cellular metabolism during plant stress responses, we treated Arabidopsis plants with prolonged darkness and examined the performance of histone Khib and H3K23ac during dark-induced starvation through metabolic profiling and transcriptome analyses. Finally, by determining the levels of Khib in several AtHDACs mutants, we identified HDA6 and HDA9 as major candidates of Khib erasers in Arabidopsis. Our results indicate that Khib is a robust histone modification mark that functions in concert with H3K23ac to regulate cellular metabolism in plants.

MATERIALS AND METHODS

Materials and growth conditions

The Arabidopsis ecotype Columbia-0 (Col-0) was used as wild-type in all experiments. The *srt1* (20), *srt2* (SALK_131994C) (21), *hda6* (22), *hda9* (23), *hda14* (24), *hda15* (25), *hda17* (26) and *hda19* (27) mutants used in this study were described previously. Arabidopsis seeds were surface sterilized with 30% bleach, sown in soil or on growth medium, and stratified at 4°C for 2 days. The seeds were grown on half-strength Murashige and Skoog medium ($\frac{1}{2}$ MS; Duchefa, Harlem, The Netherlands) agar plates, pH 5.8, in a Snijders Climate Chamber (Micro Clima) under a 16 h light/8 h dark regime with a daytime temperature at 22°C and a nighttime temperature of 20°C under a light intensity of 120 μmol m^{-2} s^{-1} for 12 days unless otherwise specified. Wild-type rice plants (*Oryza sativa* L. cv. Nipponbare) were used for analysis. Seeds were germinated in soil (Bon Sol No. 2, Sumitomo Chemical) in pots and grown for 12 days under a 14 h light/10 h dark regime at 30 °C. Maize (*Zea mays* L. cv. Canberra) and *Sorghum bicolor* (L.) Moench (BTx623) seeds were germinated in the soil in pots and grown for 12 days under a 14 h light/10 h dark regimen at 30 °C. Wild-type tobacco plants (*Nicotiana tabaccum* cv Xanthi nc) were grown in a greenhouse at 23°C for 30 days under a 14 h light /10 h dark photoperiod.

HeLa cells were cultured in Dulbecco's modified Eagle's medium (DMEM) containing 10% FBS, 1× penicillin, and streptomycin at 37°C, 5% CO_2. The cells were harvested at a density of 10^7 cells per plate for histone extraction.

For starvation and glucose feeding assays (28), seeds were sowed on $\frac{1}{2}$ MS agar medium covered with a fine nylon mesh (pore size: 45 μm) in order to facilitate the subsequent transferring operation. 14-day-old light-grown seedlings were transferred to fresh $\frac{1}{2}$ MS agar medium with no sugar or with 2% glucose. After that, seedlings on the sugar-free plates were incubated in continuous light (control) or darkness (starvation) for 5 days, while seedlings on glucose plates were incubated in the dark to serve as the glucose feeding treatment (glucose).

Histone extraction and immunoblotting

Histone fractions were extracted and enriched from human H293T cells and Arabidopsis, rice, maize, and tobacco seedlings using an EpiQuik Total Histone Extraction Kit (OP-0006-100; Epigentek) according to the manufacturers' instructions. The histone-enriched fractions were used for immunoblot analysis. Antibodies used in the immunoblotting assay included anti-H3 (ab1791; Abcam), anti-H3K23ac (ab177275; Abcam), and anti-anti-2-hydroxyisobutyryllysine (PTM-801; PTM Biolabs), whose specificity was confirmed by dot-blot assays (Supplemental Figures S1 and S2) and in a previous study (4). Peptide libraries used in this study were provided by PTM Biolabs.

Recombinant protein expression and purification

The coding sequences of Arabidopsis histone H3 (AT3G27360) and H4 (AT2G28740) were inserted into the pET28A vector (29). Recombinant protein with His-tag was expressed in *Escherichia coli* BL21 cells and purified through a Ni^{2+} Sepharose column (GE Healthcare). The primers used for cloning are listed in Supplemental Table S1.

Liquid chromatography (LC)–mass spectrometry(MS)/MS quantification of Khib levels on histones

Arabidopsis seedlings were ground in liquid nitrogen; core histones were extracted by adding 0.4 N H_2SO_4 and digesting the samples twice with trypsin. Trypsin was added at a 1:50 trypsin-to-protein mass ratio for the first digestion (overnight), and then at a 1:100 ratio for a second digestion (4 h). Lysine 2-hydroxyisobutyrylation (Khib) peptides were enriched by pre-washed antibody beads (PTM Bio-labs, Hangzhou). The eluted peptides were cleaned with C18 ZipTips (Millipore) according to the manufacturer's instructions, followed by analysis by LC–MS/MS. The MS/MS data was processed using the MaxQuant with integrated Andromeda search engine (v.1.5.2.8). Tandem mass spectra were searched against the UniProt database (https://www.uniprot.org/) concatenated with a reverse decoy database. False discovery rate thresholds for protein, peptide, and modification site were set at 1%; minimum peptide length was set at 7; the site localization probability was set at >0.75.

Chromatin immunoprecipitation (ChIP)

The ChIP experiment was performed as described (30). Approximately 2 g of leaf tissue from 12-day-old seedlings was crosslinked in 1% formaldehyde under a vacuum. Chromatin was extracted and fragmented to 200–500 bp with an ultrasonic DNA Interrupter coupled with a cold-water bath (SCIENTZ18-A, Scientz Biotechnology), and ChIP was performed using the following antibodies: 10 μg anti-Khib (PTM-801, PTM Bio-labs, Hangzhou) per IP, 5 μg anti-H3K23ac (ab177275; Abcam) per IP. The precipitated and input DNA samples were analyzed by ChIP quantitative PCR (ChIP-qPCR) with gene-specific primers listed in Supplemental Table S1. All assays were performed at least three times from two biological replicates.

ChIP-seq and data analysis

DNA from chromatin immunoprecipitation was used to construct sequencing libraries following the protocol provided by the Illumina TruSeqChIP Sample Prep Set A and sequenced on the Illumina HiSeq 3000 platform with PE 150. Low-quality reads and adapters were removed from the raw data using the Trimmomatic package (version0.35) (31), and the clean reads were mapped to the TAIR reference genome (ftp://ftp.arabidopsis.org/home/tair) using Bowtie2 (version 2.2.5) with parameters permitting < 2 mismatch. Samtools (version 0.1.19) was used to remove potential PCR duplicates, and MACS software (version 1.4.2) was used to locate enriched regions to call Khib peaks by comparing reads from the IP sample with the input sample. Wig files produced by MACS software were used for data visualization with IGV (version 2.3.88).

Metabolomic profiling and statistical analysis

Seedlings from biological triplicates (control, starvation, and glucose feeding) were freeze-dried in a vacuum freeze-dryer (Scientz-100F) and ground into a powder. 100 mg lyophilized powder was dissolved in 1.2 ml 70% methanol. The samples were mixed by vortexing for 30 s every 30 min for six times total and then stored at 4°C overnight. After being centrifugation at 12 000 rpm for 10 min, the supernatants were collected as extracts by filtration (pore size: 0.22 μm) and subjected to LC–MS/MS analysis. Global unbiased metabolic profiling was performed using a UPLC–ESI-MS/MS system (UPLC, SHIMADZU Nexera X2; MS, Applied Biosystems 4500 Q TRAP) by MetWare Biotechnology (www.metware.cn) following their standard operations.

Differential metabolites were selected based on the following parameters: 2-fold difference, $P < 0.05$. Metabolite–metabolite correlations were calculated by Pearson's product-moment correlation, and the level of significance (P-value) was measured using R statistical software.

RT-qPCR and ChIP-qPCR analysis

Total RNA was isolated from the samples using Tranzol (Transgene Biotechnology) according to the manufacturer's protocol. cDNA was prepared using All-in-One First-Strand Synthesis MasterMix (EG15133, Yugong Biolabs). RT-qPCR was performed using Taq SYBR Green qPCR Premix (EG20117, Yugong Biolabs) in an optical 96-well plate on a PRISM 7500 PCR instrument (Applied

Biosystems) using the cDNA and the products from ChIP as templates. The reactions were performed at 95°C for 10 s, 45 cycles of 95°C for 5 s, and 60°C for 40 s. Disassociation curve analysis was performed as follows: 95°C for 15 s, 60°C for 20 s and 95°C for 15 s. Data were collected using the ABI PRISM 7500 sequence detection system following the manufacturer's instructions. Relative gene expression levels were analyzed using the $2^{-\triangle\triangle CT}$ method (32). *Actin* was used as an internal control. The primers for quantitative RT-qPCR are listed in Supplemental Table S1.

RNA-seq and data analysis

RNA were isolated from the samples using TRIzol reagent (Invitrogen). The RNA-seq libraries were prepared using a Illumina TruSeq RNA Sample Preparation Kit and sequenced on the Illumina NovaSeq 6000 platform with PE150 at Annoroad Gene Technology. RNA-seq data were filtered by fastp (0.20.0) (33) to remove contamination and low-quality reads. hisat2 (2.2.0) (34) and featureCounts (2.2.0) (35) were used to map clean reads to the Arabidopsis genome (TAIR), and DESeq2 (1.0.3) (36) was used to calculate differentially expressed genes. Genes with adjusted *P*-value < 0.01 and fold change >4 under starvation treatment were considered to be differentially expressed.

Gene ontology analysis

The singular enrichment analysis tool in agriGO (37) was utilized for GO enrichment analysis of the selected gene lists, with default parameters.

RESULTS

Identification of histone lysine 2-hydroxyisobutyrylation sites in Arabidopsis

To investigate whether the histone lysine 2-hydroxyisobutyrylation (Khib) is widespread in plants, we isolated total histones from Arabidopsis, tobacco, rice and maize seedlings and performed immunoblotting; histone samples extracted from human Hela cells were used as a positive control (4). The result suggested that histone Khib is a conserved epigenomic mark in plants (Figure 1A). To support this conclusion, we examined the specificity and performance of anti-Khib antibody. The anti-Khib antibody had good specificity, as shown in dot-blot assayS (Supplemental Figures S1 and S2). We further tested the *in vivo* performance of the antibody by including recombinant Arabidopsis histones H3 and H4 as negative controls. We detected no signals for recombinant histones H3 and H4, in parallel with the Arabidopsis control, which had obvious bands (Supplemental Figure S3), confirming the reliability of the immunoblotting signals detected in plants (Figure 1A).

We then performed a mass spectrometry-based assay to identify histone Khib sites in Arabidopsis. A total of 41 Khib sites were present throughout both the N tails and core regions of the histones (Figure 1B and Supplemental Figure S4 and Table S2). We noticed that the Arabidopsis histone Khib pattern largely resembled that of human and mouse (4) but still with species-specific modification sites, for instance, H3K53 and H4K12 were present only in Arabidopsis (Figure 1b and Supplemental Table S2). Many Khib sites recognized in rice and moss (7,8) were also present in Arabidopsis, suggesting that Khib is a highly conserved histone mark in plants. Most strikingly, the absence of several khib sites at the very end of the N-tail regions of H3 (H3K4, H3K9, H3K14 and H3K18) and H4 (H4K5, H4K8 and H4K16) represent the largest differences between mammals and plants (Figure 1B and Supplemental Table S2). In addition, 14 of the 41 Khib sites were uniformly distributed on H2B in Arabidopsis, which would likely alter the association of H2B and its coupling DNA strands via the transition from a positive state (with a protonated amine group) to a neutralized state (with Khib) (4) (Figure 1B and Supplemental Table S2). Together, these results indicate plants and mammals have their preferential Khib sites, especially on the most conserved histones (H3 and H4), implying that Khib is a conserved yet diverse histone mark between plants and mammals.

Comparative analysis of histone Khib and other epigenomic marks in Arabidopsis

To probe the role of histone Khib in Arabidopsis chromatin, we performed chromatin immunoprecipitation-sequencing (ChIP-seq) assays using anti-Khib antibody in 12-day-old wild-type seedlings. In total, 17 974 and 12 773 Khib peaks were recognized, respectively, in two replicates of ChIP-seq that showed high Pearson correlation coefficients (>0.9 according to reads). Among these, 10 238 ($>80\%$ in the case of replicate 2) overlapped, indicating that the data are reliable and reproducible (Supplemental Figure S5a and c and Table S3). The histone acylation modifications were widely distributed in the Arabidopsis genome. In addition, the ChIP-seq data were validated by ChIP-qPCR tests on five randomly selected Khib-modified genes and five randomly selected genes not modified by Khib (Supplemental Figure S6a and b). Together, the analysis provided a chromatin landscape of the distribution of histone Khib sites in Arabidopsis.

In detail, approximately 35% of protein-coding genes, only 7% of transposable element (TE)-related genes and 2% of transposable elements and repeats were marked by Khib; we designated these as Khib-modified genes (Figure 2A). We then determined Khib peak distribution over different regions of protein-coding genes. The modifications were highly enriched at the transcription start sites (TSSs) of protein-coding genes compared to TE-related genes (Figure 2B). To investigate whether histone Khib-enrichment at the TSS was correlated with gene transcription, we performed RNA-seq analysis to obtain genome-wide gene expression patterns (Supplemental Table S4). All protein-coding genes were classified into five groups based on their expression levels (38). Actively expressed genes (top 20% and 21–40%) showed significantly higher levels of histone Khib compared to moderately expressed genes (41–60%), whereas genes expressed at low levels showed depletion of this mark across the entire gene body (Figure 2C). To validate the RNA-seq data, we measured the transcript levels of 10 randomly selected genes by RT-qPCR, showing that transcripts of five Khib-modified genes accumulated at higher levels com-

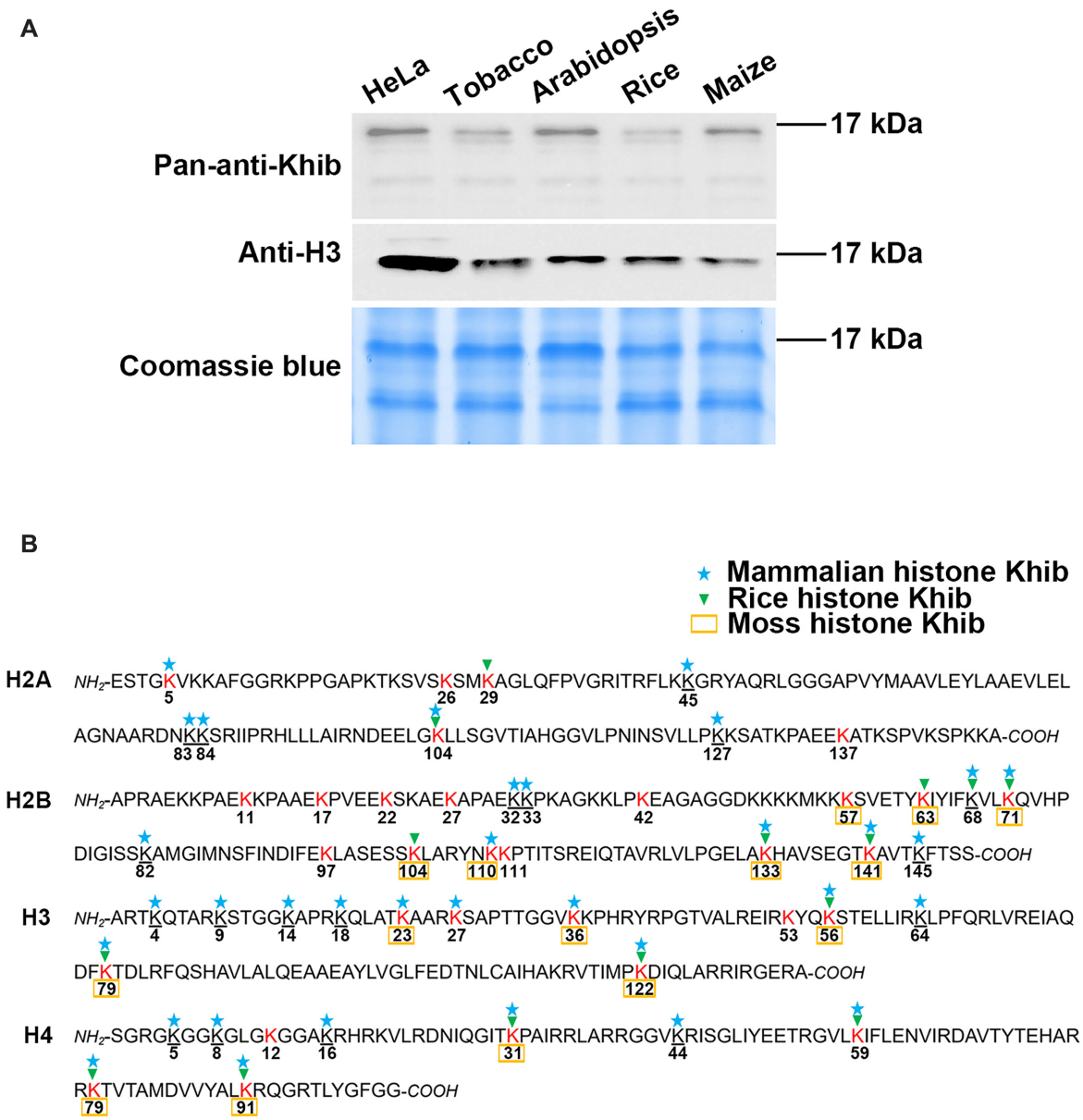

Figure 1. Identification of Arabidopsis histone Khib modifications. (**A**) Immunoblotting of Khib in histones isolated from human Hela cells, and of Arabidopsis, rice, maize and tobacco seedlings. Coomassie blue staining of total histone is shown below. See Materials and Methods for details about the cultures and sample collections. (**B**) Identification of Arabidopsis histone Khib sites by mass spectrometry (see Supplemental Figure S4 and Supplemental Table S2). The Khib sites in Arabidopsis (red letters), rice (green triangles), moss (yellow rectangles) and mammals (blue stars) are shown. The lysines that are underlined and marked by blue stars are unique mammalian sites.

pared to those of five Khib-unmodified genes (Supplemental Figure S6c). By contrast, histone Khib levels were very low in TE-related genes (Figure 2A and B). These results suggest that the histone Khib enrichment level is a positive determinant of gene transcript abundance.

Analysis of a correlogram of histone Khib with known epigenomic marks demonstrated that Khib was highly correlated with the active histone marks H3ac, H4ac and H3K4me2/3, which are primarily found in euchromatin, and not with the inactive, heterochromatic modifications H3K9me2, H3K27me1 and 5mC (39) (Supplemental Figure S7 and Table S5). Furthermore, the highest correlation was observed between Khib and the noncanonical histone mark H3K23ac (Figure 2D). Overall, the genomic and genic distributions of Khib appear to be somewhat similar to that of H3K23ac (Figure 2A; Supplemental Figure S8). Collectively, this analysis supports the notion that Khib acts as an active chromatin mark in Arabidopsis.

Co-enrichment of Khib and H3K23ac is correlated with high gene expression levels

We identified 9350 Khib-marked Arabidopsis genes in this study, 8006 of which (85.6%) were also marked by H3K23ac, accounting for half (8006 out of 15 139) of H3K23ac-marked genes (Figure 3A). We quantitatively de-

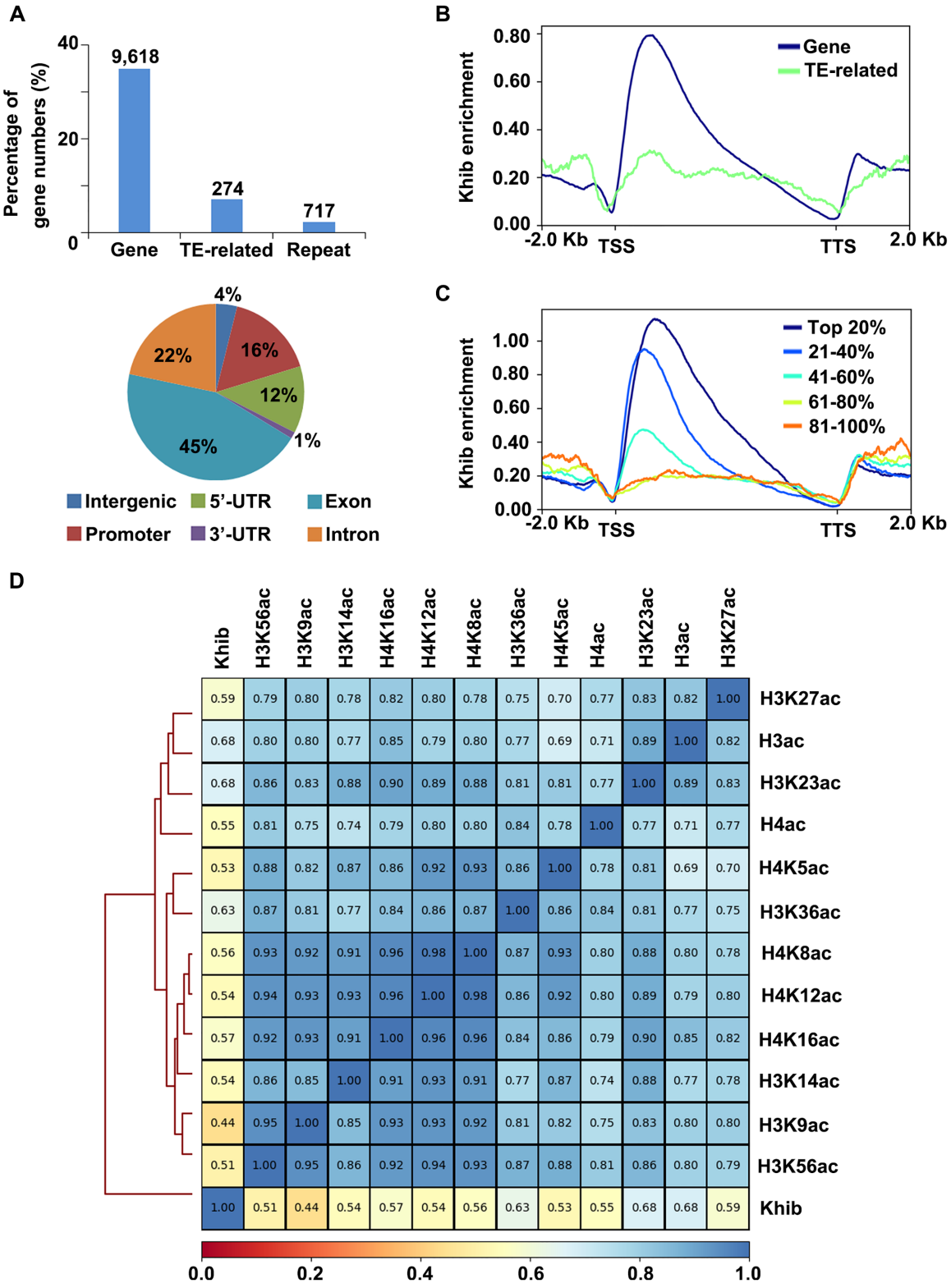

Figure 2. Distribution of histone Khib modifications in the Arabidopsis genome. (**A**) Top, proportions of Khib-marked protein-coding genes, transposable element (TE)-related genes, and transposable elements and repeats; bottom, distribution of Khib peaks at different genic and intergenic regions. UTR, untranslated region. (**B**) Average genome-wide occupancies of Khib in protein-coding genes and TE-related genes. The 2-kb upstream and downstream flanks were aligned. The *x*-axis represents genes from the transcription start site (TSS) to the transcription termination site (TTS). The *y*-axis represents the value of ChIP enrichment normalized to the input. (**C**) Metaplot showing that Khib level is positively correlated with gene expression level. 'Top 20%' represents the gene group with the highest expression levels. (**D**) Correlogram of Khib and other histone modifications. The genome was divided into 10-kb bins, and the average values of each bin were used to calculate Pearson correlation coefficients (represented by colors).

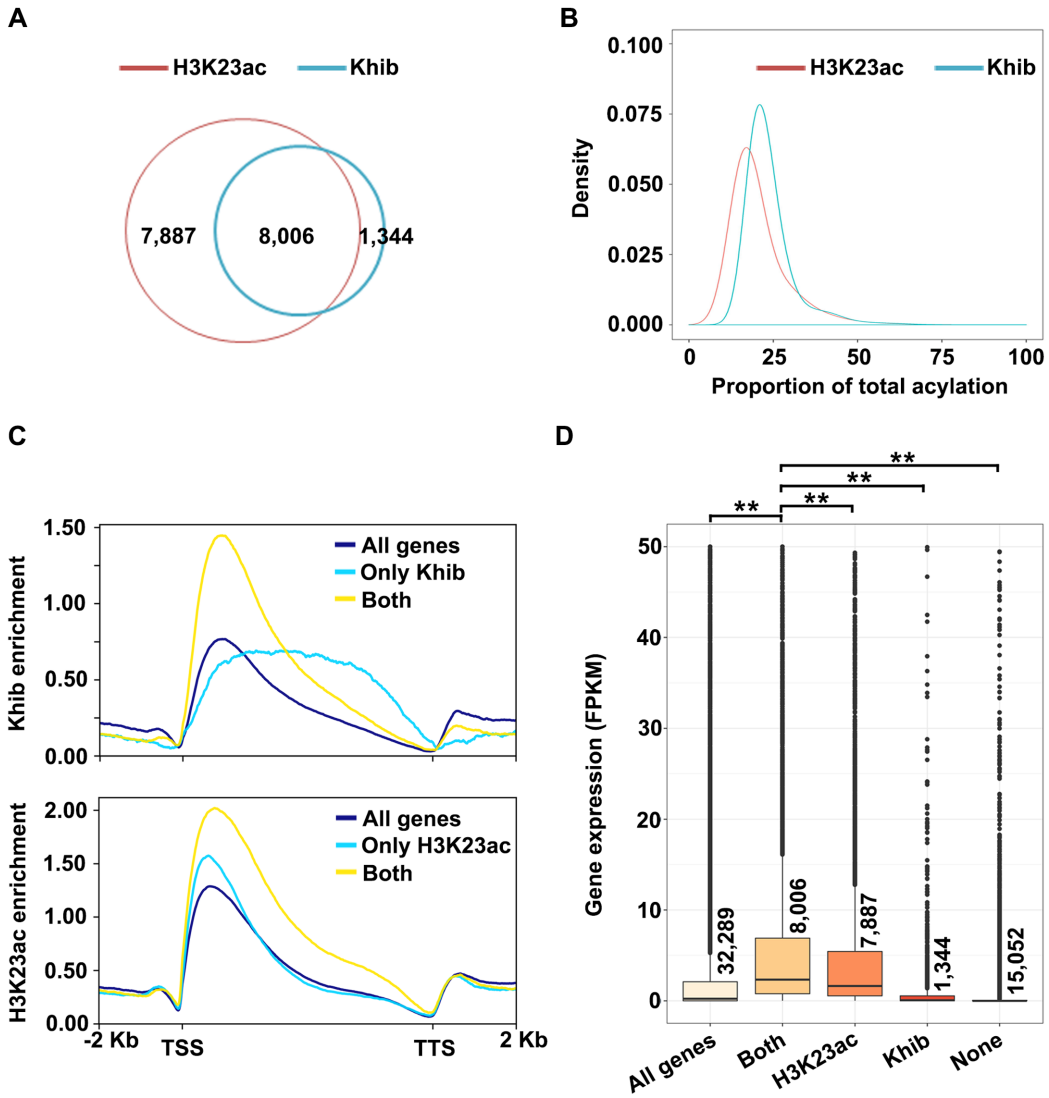

Figure 3. Different combinations of Khib and H3K23ac modifications affect gene expression. (**A**) Venn diagram of Khib- and K3K23ac- marked genes. (**B**) Density curve of the proportion of Khib/H3K23ac modifications in all genes. (**C**) Average genome-wide occupancies of Khib and H3K23ac in all genes ($N = 32{,}289$), genes with only Khib ($N = 1{,}344$), and genes with only H3K23ac ($N = 7887$). (**D**) Box plots of the expression levels of genes marked by Khib and H3K23ac alone or both compared to those without the two marks. The five statistical values in the boxplot from top to bottom are the maximum, third quartile, median, first quartile and minimum. The asterisks (**) indicate significant differences at $P < 0.01$ (two-sided Wilcoxon rank sum tests) from biologically independent ChIP–seq and RNA-seq experiments.

termined the modification densities of Khib and H3K23ac compared to the proportion of total acylation in the marked genes, finding that the proportion for H3K23ac varied in a wider range than that of Khib (Figure 3B). These results indicate that H3K23ac is more dynamic than Khib and that Khib might contribute to the H3K23ac-regulated active chromatin state. We then explored the genome-wide occupancies of Khib and H3K23ac. Khib was more abundant in the gene body region, and the addition of Khib magnified the H3K23ac enrichment levels in both Khib- and H3K23ac-modified genes (Figure 3C).

To unveil the potential roles of Khib in regulating gene expression, we analyzed expression levels of genes modified by combinations of the two marks to investigate the functional relationship between Khib and the closely concurrent H3K23ac (Figure 3D; Supplemental Table S4). Genes marked by H3K23ac had higher expression levels than genes marked only by Khib, and genes marked by both PTMs showed higher expression than genes marked by Khib or H3K23ac alone (Figure 3D). These results suggest that the combined enrichment of Khib and H3K23ac is correlated with high gene expression; in other words, Khib and H3K23ac may act in combination to promote gene expression activity. Collectively, our results strengthen the notion that Khib acts as an epigenomic mark that is complementary to H3K23ac in Arabidopsis.

Khib- and H3K23ac-marked genes are ubiquitously expressed

To further characterize Khib modification, we asked whether there are any unique patterns of Khib and H3K23ac during plant development. We included previously reported RNA-seq datasets of various tissues from

different developmental stages (Supplemental Table S5) to examine the dynamic expression patterns of genes in four clusters: (i) genes marked with both Khib and H3K23ac, (ii) genes not marked with Khib or H3K23ac, (iii) genes marked only with H3K23ac and (iv) genes marked only with Khib. Approximately 86% of genes (6813 out of 7854) containing both Khib and H3K23ac showed a globally high expression level (expression levels; $\log_{10}(TPM + 1) > 3$) across all tissue types (Figure 4 and Supplemental Figure S9). By contrast, genes depleted in both Khib and H3K23ac ('None' cluster) had generally low expression levels in all tissues (Figure 4). Intriguingly, whereas the vast majority of 'H3K23ac only' genes showed high expression levels in all tissues, only a small set of the 'Khib only' genes exhibited active expression (Figure 4).

To further confirm the tissue-specific expression patterns of Khib- and H3K23ac-marked genes, we calculated the significance value of tissue specificity for each gene cluster at all developmental stages and in all tissue types using the TissueEnrich R package (40). Interestingly, genes containing both Khib and H3K23ac displayed relatively high tissue-specificity in seedling, callus tissue, shoots, and all vegetative organs, which is similar to the expression patterns of genes marked only with H3K23ac (Supplemental Figure S10). Meanwhile, genes marked only with Khib and genes with no Khib or H3K23ac marks tended to be active in reproductive organs, such as bud, silique, and inflorescence tissue (Supplemental Figure S10). Taken together, these results suggest that the presence of both Khib and H3K23ac is associated with highly and ubiquitously expressed genes and that Khib and H3K23ac coordinately regulate seedling development during the vegetative stage.

To reveal Khib-mediated biological processes, we performed Gene ontology (GO) analysis. The GO terms transporter activity and catalytic activity were overrepresented in genes marked only with Khib, whereas genes marked with both Khib and H3K23ac were predominantly enriched in GO terms response to stimulus, cellular processes, and metabolic process (FDR < 0.0001) (Supplementary Table S6). In addition, the carbohydrate-related pathway was enriched in the only Khib-marked low expressed genes (FDR < 0.001; Supplemental Figure S11). The substrates for histone acetylation/acylation, such as acetyl-CoA, butyryl-CoA, and crotonyl-CoA, are important primary metabolites which are sensitive to cellular stress responses (41). Altogether, these data indicated that histone Khib and H3K23ac may act together to influence plant stress responses and to coordinate cellular metabolic processes.

Histone Khib and H3K23ac are co-enriched on genes involved in prominent metabolic pathways in plant responses to dark-induced starvation

Light not only functions as the energy source used to produce carbohydrates (sugars), but also is a crucial environmental signal for plant growth and development (42,43). Starvation stress due to prolonged darkness is thought to dramatically affect primary carbohydrate metabolism in plants (11), and it activates the low-energy response in Arabidopsis (28). Therefore, we investigated the performance of histone Khib and H3K23ac in response to starvation. We subjected 14-day-old Arabidopsis seedlings to darkness for 5 days and divided them into two groups: plants in the starvation group were grown on sugar-free plates, while plants in the glucose feeding group were supplied with glucose in the medium. Immunoblotting showed that the overall histone Khib level decreased under starvation and was restored by glucose treatment compared to the control (Figure 5A), suggesting that starvation affects histone Khib due to dark-induced carbon deficiency.

This finding to some extent resembled the observation in yeast (5). As noted above, however, darkness may trigger much more complex intracellular stress processes in autotrophic plants than in yeast. In other word, it seemed possible that the conserved marks have broader functional roles in plants than in yeast. To investigate this, we identified starvation-responsive genes marked by both histone Khib and H3K23ac by monitoring their gene expression and modification levels using an integrative transcriptomic and metabolic-based strategy. Under starvation, 792 genes showed >4 fold up-regulation and 3252 genes showed >4 fold downregulation compared to the control (P-value $<$ 0.01) (Figure 5B and C; Supplemental Figure S12 and Table S7). GO analysis revealed that the downregulated genes were significantly enriched in multiple pathways, such as response to stimulus, cellular process, and metabolic process, whereas the upregulated genes were only enriched in response to stimulus (Supplemental Table S8). In response to glucose feeding, 1128 genes displayed >4-fold upregulation and 162 genes showed >4-fold downregulation (P-value < 0.01) comparing to genes in plants under starvation conditions (Supplemental Figure S12), demonstrating that 34.7% of the dark-repressed genes (1128 out of 3252) restored their activities in response to glucose feeding. These data suggest that these genes are directly responsive to starvation stress. Interestingly, Kyoto Encyclopedia of Genes and Genomes (KEGG) pathway analysis of these differentially expressed genes revealed that starch and sucrose metabolism, pentose and glucuronate interconversions, and phenylpropanoid biosynthesis were the most significantly enriched metabolic pathways among primary starvation responses (Figure 5d; Supplemental Figure S13; Supplemental Table S9).

We performed global metabolic profiling to identify 763 differential metabolites under control, starvation, and glucose feeding conditions (Supplemental Table S10). To couple these results with the results of transcriptomic analysis, we performed similar comparisons among different treatments. We observed obvious changes in the contents of specific metabolites, including alkaloids, amino acids and derivatives, flavonoids, lignans and coumarins, organic acids, and saccharides and alcohols (Figure 5E; Supplemental Table S10). To further probe the metabolite dataset, we performed correlation analysis of the detected metabolites to uncover their relationships and underlying mechanisms using Pearson's product-moment correlation. Negative correlations were found in the same cluster of compounds (in particular amino acids and derivatives, and flavonoids), as well as metabolites of amino acids and derivatives against flavonoids and lipids and metabolites of flavonoids against lipids (Supplemental Figure S14 and Table S11). In addition, compared to control and glucose feeding conditions,

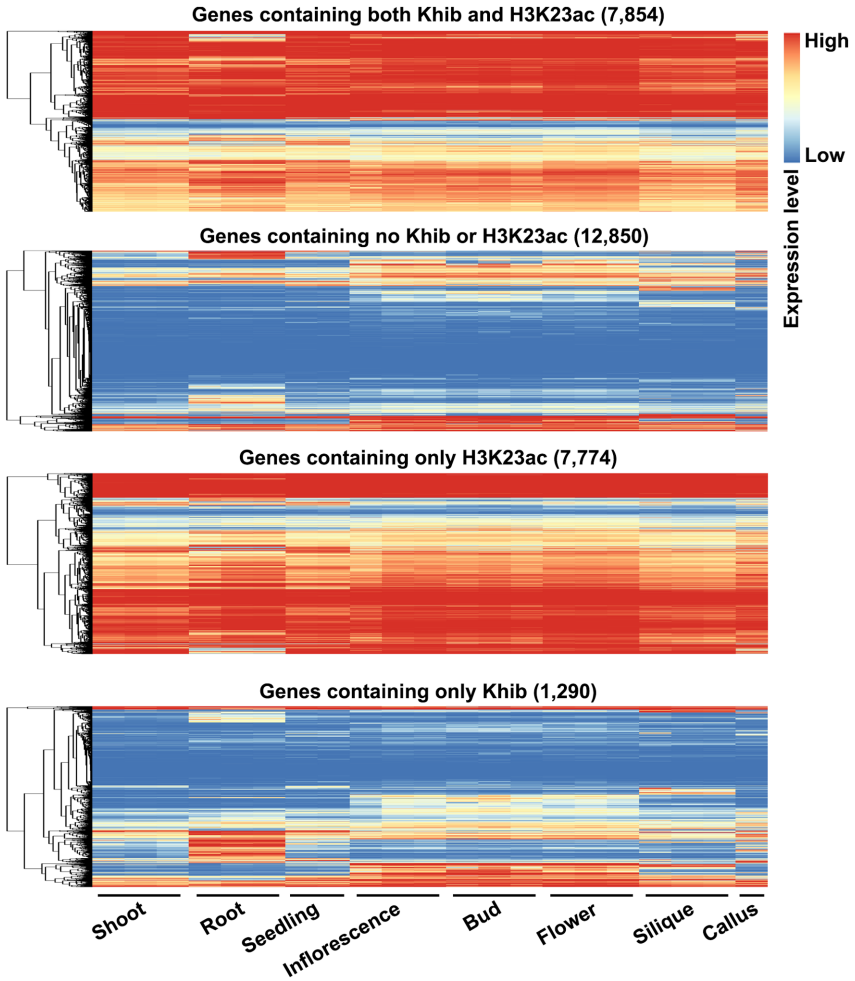

Figure 4. Genes marked with both Khib and H3K23ac are ubiquitously expressed. Heatmaps showing the expression patterns of four gene clusters (defined in Figure 3D) in tissues at different developmental stages. Red represents a high gene expression level and blue represents a low gene expression level (log_{10}(TPM+1)). For each sample, three or two biological replicates of RNA-seq data are shown, depending on the original source.

starvation conferred the greatest variation in metabolite–metabolite correlations (Supplemental Figure S14 and Table S11), supporting the notion that dark-induced starvation is a prominent stress condition that interrupts cellular metabolic processes. Accordingly, the contents of starch and sucrose intermediates changed upon starvation and glucose feeding. Among these, trehalose and sucrose levels decreased upon starvation but were restored by glucose feeding, whereas D-glucose-6P, α-D-glucose-1P and D-fructose-6P accumulated in response to starvation. In addition, when we examined the changes in levels of seven phenylpropanoid intermediates, the levels of *p*-coumaryl alcohol, coniferyl alcohol, and coniferin decreased in response to starvation and were restored by glucose feeding, whereas phenylalanine, cinnamic acid, *p*-coumaroylquinic acid and sinapoyl choline exhibited the opposite tendencies. The metabolic profiling prompted us to investigate the activities of the associated metabolism-related genes.

Considering that the activities of enzyme-encoding genes are associated with the levels of the related compounds, exploring the correlation of histone modifications with the expression activities of target genes could pave the way toward a better understanding of the metabolic roles of histone Khib and H3K23ac in the response to dark-induced starvation. Thus, we targeted the following genes: three genes encoding starch and sucrose metabolic enzyme, *GRANULE BOUND STARCH SYNTHASE 1* (*GBSS1*), *SUCROSE SYNTHASE 6* (*SUS6*), and *TREHALASE 1* (*TRE1*); and five phenylpropanoid biosynthesis-related genes, *PHENYLALANINE AMMONIA-LYASE 1* (*PAL1*), *4-COUMARATE:COA LIGASE 1* (*4CL1*) and (*4CL5*) and *UDP-GLUCOSYL TRANSFERASE 72E1* (*UGT72E1*) and (*UGT72E3*). We verified their expression patterns obtained by RNA-seq through RT-qPCR (Figure 5f and Supplemental Figures S15–S17 and Table S12), revealing that their expression was repressed by starvation but restored by glucose feeding, with the exception of *TRE1*. More importantly, a ChIP-qPCR assay supported the proposal that the modification levels of both histone Khib and H3K23ac at TSS regions are positively correlated with the expression levels of their genes (Figure 5g and h). Together, our data suggest that histone Khib and H3K23ac are co-enriched on genes involved in sugar metabolism and phenylpropanoid biosynthesis and

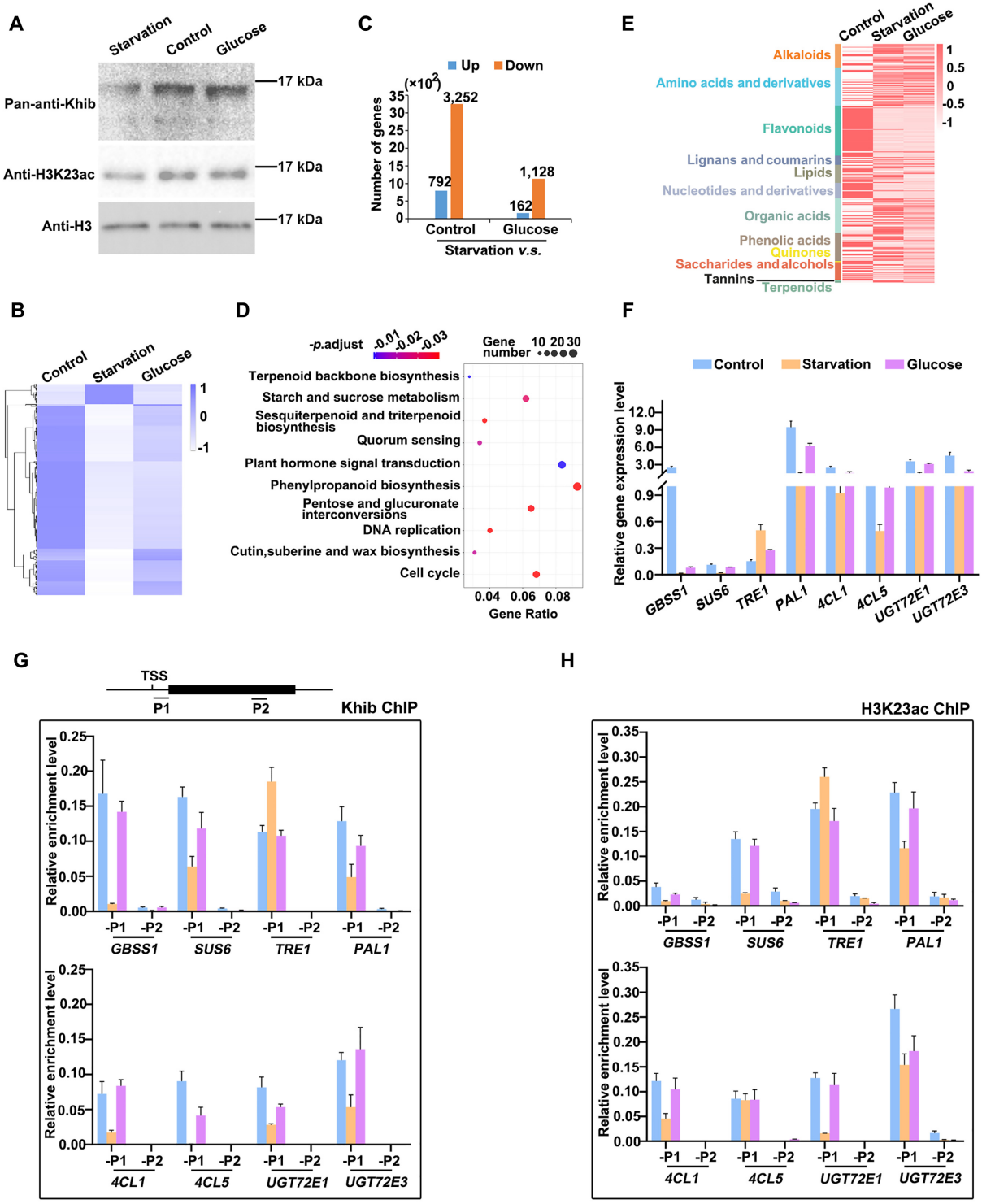

Figure 5. The roles of histone Khib and H3K23ac in cooperatively fine-tuning cellular metabolic pathways during plant responses to dark-induced starvation. (**A**) Immunoblotting showing the changes in histone Khib and H3K23ac in response to different treatments: control (light, no glucose), starvation (dark, no glucose), or glucose feeding in the dark (glucose). (**B**) Overall cluster analysis and heatmap of differentially expressed genes (DEGs). The color bar denotes gene expression levels calculated by FPKM. (**C**) Summary of DEGs. (**D**) Kyoto Encyclopedia of Genes and Genomes (KEGG) pathway enrichment analysis of overlapping DEGs. The *y*-axis represents the pathway category and the *x*-axis represents the degree of enrichment of the pathway (Gene ratio, number of differently expressed genes in a given pathway divided by the total number of genes involved in that pathway). Circle color indicates the *Q* value (corrected *P*-value) and circle size indicates the number of involved genes. Significant enrichment was detected at $Q < 0.05$. The top 10 pathways with the smallest *Q* values are shown. (**E**) Heatmap showing the changes in the contents of metabolites under control, starvation, and glucose conditions. Metabolites were categorized according to compound classes. *P*-values are shown in Supplemental Table S10. (**F**) qRT-PCR analysis of relative gene transcript levels compared to the reference gene *Actin*. Bars are means ± SD from biological triplicates. (G and H) ChIP-qPCR analysis of anti-Khib enrichment (**G**) and anti-H3K23ac enrichment (**H**). Bars are means ± SD from three biological replicates.

thereby serve to fine-tune plant responses to dark-induced starvation.

HDA6 and HDA9 are involved in erasing histone Khib marks in Arabidopsis

Mammalian sirtuin (SRT) and Zn-finger Histone deacetylases (HDAC) have debutyrylase and/or decrotonylase activities (44). In particular, Human HDAC2 and HDAC3 were recently identified as Khib deacylases (6). To determine whether (and which) HDAC proteins regulate histone Khib in Arabidopsis, we analyzed *SRT* and *AtHDA*-related T-DNA mutants by immunoblotting with anti-Khib antibody. Compared to wild-type plants and the loss-of-function mutants of *srt1*, *srt2*, *hda14*, *hda15*, *hda17* and *hda19* (Supplemental Figure S18), we observed an obvious increase in Khib band intensity in *hda6* and *hda9* (Figure 6). Phylogenetic study suggested that *AtHDA6* and *AtHDA9* are homologous genes of human *HDAC2* and *HDAC3* (45), which belong to the eukaryotes RPD3/HDA1 class I family. Consistently, when a comparison of the enrichment profiling of Khib and a previously reported HDA9 ChIP-seq dataset (46), clearly demonstrated that Khib was not present in a large portion of HDA9 enriched genes (5475 out of 11 914), and the enrichment patterns of Khib and HDA9 overlapped to some extent (Supplemental Figure S19). Collectively, the immunoblotting results suggest that AtHDA6 and AtHDA9 have deacylase activity to erase Khib in Arabidopsis.

DISCUSSION

Due to advance in mass spectrometry (MS)-based technologies, a large number of histone PTMs and their roles have been revealed in recent years. In particular, short-chain lysine acylation has emerged as a new type of PTMs affects gene expression and may be functionally different from histone Kac (47). A recent genome-wide study of the two typical histone lysine acylations, Kbu and Kcr, together with H3K9ac, suggested that histone acylation and acetylation interact to regulate primary metabolism by altering gene expression in rice (19). However, less is known about the role of Khib in higher plants.

Here, we present a genomic view of histone Khib modification in Arabidopsis. We identified 41 histone Khib sites in Arabidopsis, considerably more than have been detected in rice (16 sites) (8) or moss (20 sites) (7). We attribute this difference to improved detection due to the use of purified histone proteins as the mass spectrometry (MS) input. The histone Khib sites identified in Arabidopsis present a genomic view of histone Khib modification in plants. Notably, we observed a few unique features of plants as compared to mammalian histone Khib. Whereas Kac is enriched at the N-tail sites of H3 and H4 (e.g. H3K4, H3K9 and H4K8) in all known eukaryotes, and mammalian histone Khib occupies most Kac sites (4), the plant histone Khib sites were almost absent from these major well-known N-tail lysines and preferentially resided at the core histone regions. The speculation that Khib and other acylations could potentially compete with histone Kac in mammals prompted questions about what determines and coordinates the presence of histone acetylation and short-chain acylations, as well as their functional interplay (48). Interestingly, H3K56 and H3K79, which are free of acetylation in Arabidopsis (49), are exclusively occupied by the Khib mark. Overall, it appears that plants use a more sophisticated method to avoid any competition with Kac at N-tails and that their interplay should be easily captured. More interestingly, H3K53 and H4K12 represent unique plant-specific Khib sites. In addition, one-third of the 41 Khib sites in Arabidopsis were uniformly distributed on the less conserved histone H2B (50), where they are likely to alter the association of H2B and its coupling DNA strands via the transition from a positive state (with the protonated amine group) to a neutralized state (with Khib) (Figure 1b and Supplemental Table S2).

However, before drawing a solid conclusion, it is worth noting that the specificity of the pan-anti-Khib antibody may affect its performance in plants. The first reported study of histone Khib marks in mammals included a dot-blot assay validating that the antibody used had good specificity (4). In this initial study, nine peptide libraries comprising sequences with lysine modifications by diverse short-chain fatty acids, such as Kac, Kbu, Kcr, Khib and an unmodified lysine (negative control) were used for comparison in the dot-blot immunoreaction (4). Our dot-blot assay also suggested the anti-Khib antibody used in this study had good specificity (Supplemental Figure S1). In addition, we tested the *in vivo* performance of the antibody by including recombinant Arabidopsis histones H3 and H4 as negative controls (Supplemental Figure S3), confirming that the immunoblotting signals detected in plants were reliable. Plant researchers often have to counter the limitations of using antibodies against conserved proteins or modifications, and in cases this does not pose a barrier (19). In conclusion, these data demonstrate that the distribution of histone Khib appears is diverse between plants and mammals, suggesting that the histone Khib mark may play unique roles in plant epigenetics.

Thus far, global profiling of the Khib proteome has been reported in mammalian cells (6), yeast (5), rice (8) and moss (7), revealing diverse non-histone Khib protein substrates that play functional roles in multiple primary metabolic processes, such as the glycolysis/gluconeogenesis pathway (5), starch biosynthesis pathway, and lipid metabolism (8), as well as responses to various biotic and abiotic stresses (5,6). However, whether and to what extent this histone epigenetic mark affects gene expression and how it is regulated in plants have remained elusive. To address this question, we performed genome-wide enrichment profiling of histone Khib via ChIP-seq in Arabidopsis. The modifications were highly enriched at the TSSs of protein-coding genes and were positively correlated with gene expression (Figure 2a and b), suggesting that the histone Khib is an active epigenomic mark. This conclusion was further confirmed by ChIP-qPCR.

To decipher the roles of Khib in regulating gene expression, we investigated the correlations between the distribution of Khib and those of other chromatin features. Khib was highly correlated with the active histone mark Kac. Among these chromatin features, the highest correlation was with H3K23ac (Figure 2; Supplemental Figure S7). In addition, the combined enrichment of Khib and H3K23ac was correlated with high gene expression levels, suggest-

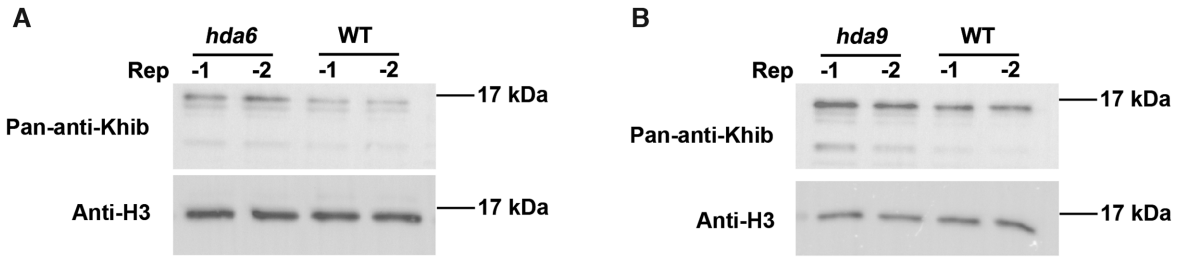

Figure 6. HDA6 and HDA9 promote deacylation in Arabidopsis. (A and B) Histone Khib levels in *hda6* (**A**) and *hda9* (**B**) mutants compared to wild type (WT) as determined by immunoblotting. Two biological replicates were loaded in the blots for each sample.

ing that these marks generally act in concert to maintain high transcriptional outputs during plant development. Histone tail modifications influence the deposition of other modifications (51), for instance, H3K14 pre-acetylation is one determinant to anti-silencing factor 1 (Asf1)-mediated H3K56ac in yeast (52). Our finding raised the fundamental question that whether N-tail Kac modifications determine the deposition of Khib. Khib could mark active genes in a similar manner to Kac in mammals, suggesting it might function under specific circumstances where histone acetylation would not function properly (48). However, the situation in plants may not be parallel to that in mammals. In particular, our findings support the notion that Kac and Khib act in combination instead of functioning reciprocally.

Given that the enrichment of Khib is sensitive to cellular glycolysis (5), we explored the roles of Khib in Arabidopsis growing in prolonged darkness. Our data demonstrate that the starvation-induced loss of overall histone Khib and H3K23ac enrichment could be restored after glucose feeding in a synergistic manner (Figure 5a). Together with the results of GO analysis of co-marked genes (Supplemental Figure S11), this observation suggests that glycolysis and carbon metabolism are common central metabolic processes that are affected by these conserved marks across species. Our metabolic profiling data integrated with transcriptome data reveal that dynamic metabolic alterations related to Khib and H3K23ac mainly occur in starch and sucrose metabolism, pentose and glucuronate interconversions, and phenylpropanoid biosynthesis in response to starvation (Figure 5).

Histone Khib and H3K23ac synergistically modify and de-modify these key enzyme-encoding genes (Figure 5) to affect their expression, thereby fine-tuning plant responses to dark-induced starvation. We reasoned that the accumulation of D-glucose-6P and α-D-glucose-1P (two intermediates of starch and sucrose biosynthesis) upon starvation could possibly be attributed to the reduced activity of their downstream starch synthase and granule-bound starch synthase GBSS1, whereas the reduced sucrose production upon starvation could be due to the reduced activity of its upstream sucrose synthase SUS6. Accordingly, the levels of histone Khib and H3K23ac enrichment on these enzyme-encoding genes changed and were positively correlated with their expression (Figure 5). On the other hand, phenylpropanoids are involved in many aspects of plant responses to biotic and abiotic stimuli, and they represent sources of numerous secondary metabolites, including lignin, stilbenes, and flavonoids (53,54). Notably, genes marked by both histone Khib and H3K23ac (such as gene members of *PAL*, *4CL* and *UGT72E*; Figure 5; Supplemental Table S12) function in phenylpropanoid biosynthesis, and their activities are associated with the contents of the precursor phenylalanine and a few intermediates (Figure 5). Thus, the influence of these two marks may extend well beyond those we have identified here. Even though our analysis merely provided a glance of sugar metabolism and phenylpropanoid pathways under starvation conditions, it revealed that these two histone marks function in concert to regulate cellular metabolism in Arabidopsis during stress responses.

Mounting evidence suggests that histone HATs and HDACs are the major enzymes that reversibly incorporate and remove lysine acetylations as well as several types of acylation (44). Consistent with findings in humans (6), our findings suggest that AtHDA6 and AtHDA9, the closest homologs of human HDAC2 and HDAC3 have *in vivo* deacylase activity that serves to erase Khib in Arabidopsis. HDA6 and HDA9 are involved in many developmental processes and stress responses in plants (15,55). Interestingly, HDA9 regulates the transcriptional activities of autophagy-related genes to mediate plant autophagy in response to the light-to-dark conversion (56), while it negatively regulates plant immunity (57) as well as salt and drought stress responses (58). HDA6 also represses pathogen defense responses in Arabidopsis (59). A previous study pointed to a potential link between HDA6- and HDA9- mediated histone deacetylase metabolism by analyzing their participation in brassinosteroid signaling (60). Based on these findings, we plan to investigate whether and how these histone deacetylases affect the histone modifications Khib and Kac to regulate other stress responses in plants. In conclusion, our study sheds light on the characteristics and roles of the recently discovered active histone mark Khib in plant development and adaptation.

DATA AVAILABILITY

The raw sequence data of ChIP-seq reported in this paper have been deposited in Sequence Read Archive (SRA), under accession number PRJNA734459. The raw sequence data of RNA-seq have been deposited in Sequence Read Archive (SRA), under accession number PRJNA720835. The mass spectrometry proteomics data have been uploaded onto the ProteomeXchange Consortium via the PRIDE partner repository with the dataset identifier of PXD018017.

Sequence data from this article can be found in the Arabidopsis Genome Annotation website (https://www.arabidopsis.org/) under the following accession numbers: *SRT1*, AT5G55760; *SRT2*, AT5G09230; *HDA6*, AT5G63110; *HDA9*, AT3G44680; *HDA14*, AT4G33470; *HDA15*, AT3G18520; *HDA17*, AT3G44490; *HDA18*, AT5G61070; *GBSS1*, AT1G32900; *SUS6*, AT1G73370; *TRE1,* At4g24040; *PAL1*, AT2G37040; *4CL1*, AT1G51680; *4CL5*, AT3G21240; *UGT72E1*, AT3G50740; *UGT72E3*, AT5G26310.

SUPPLEMENTARY DATA

Supplementary Data are available at NAR Online.

ACKNOWLEDGEMENTS

We thank Dr Xiang Wang for providing human cell lines and Dr Kun Meng for assisting us with protein expression and purification.

FUNDING

National Science Foundation of China [32000609, 31900427, 31801210]; Principle Investigator Program [HBMUPI202104]; Science Research and Development Project of Shiyan [2021K20]; Cultivating Project for Young Scholar [2017QDJZR26] at Hubei University of Medicine; Natural Science Basic Research Program of Shaanxi [2020JC-29]; Project of Youth Talent in Hubei Provincial Department of Education [Q20191207, C.Z]; Open Project of Hubei Key Laboratory of Wudang Local Chinese Medicine Research (Hubei University of Medicine) [WDCM2019009, C.Z.]; Initial Project for High-Level Personnel of China Three Gorges University to C.Z. Funding for open access charge: National Science Foundation of China.
Conflict of interest statement. None declared.

REFERENCES

1. Azevedo,C. and Saiardi,A. (2016) Why always lysine? The ongoing tale of one of the most modified amino acids. *Adv. Biol. Regul.*, **60**, 144–150.
2. Kebede,A.F., Nieborak,A., Shahidian,L.Z., Le Gras,S., Richter,F., Gomez,D.A., Baltissen,M.P., Meszaros,G., de Fatima Magliarelli,H. and Taudt,A. (2017) Histone propionylation is a mark of active chromatin. *Nat. Struct. Mol. Biol.*, **24**, 1048.
3. Chen,Y., Sprung,R., Tang,Y., Ball,H., Sangras,B., Kim,S.C., Falck,J.R., Peng,J., Gu,W. and Zhao,Y. (2007) Lysine propionylation and butyrylation are novel post-translational modifications in histones. *Mol. Cell. Proteomics*, **6**, 812–819.
4. Dai,L., Peng,C., Montellier,E., Lu,Z., Chen,Y., Ishii,H., Debernardi,A., Buchou,T., Rousseaux,S. and Jin,F. (2014) Lysine 2-hydroxyisobutyrylation is a widely distributed active histone mark. *Nat. Chem. Biol.*, **10**, 365.
5. Huang,J., Luo,Z., Ying,W., Cao,Q., Huang,H., Dong,J., Wu,Q., Zhao,Y., Qian,X. and Dai,J. (2017) 2-Hydroxyisobutyrylation on histone H4K8 is regulated by glucose homeostasis in Saccharomyces cerevisiae. *Proc. Natl. Acad. Sci. U.S.A.*, **114**, 8782–8787.
6. Huang,H., Luo,Z., Qi,S., Huang,J., Xu,P., Wang,X., Gao,L., Li,F., Wang,J. and Zhao,W. (2018) Landscape of the regulatory elements for lysine 2-hydroxyisobutyrylation pathway. *Cell Res.*, **28**, 111.
7. Yu,Z., Ni,J., Sheng,W., Wang,Z. and Wu,Y. (2017) Proteome-wide identification of lysine 2-hydroxyisobutyrylation reveals conserved and novel histone modifications in Physcomitrella patens. *Sci. Rep.*, **7**, 15553.
8. Meng,X., Xing,S., Perez,L.M., Peng,X., Zhao,Q., Redoña,E.D., Wang,C. and Peng,Z. (2017) Proteome-wide analysis of lysine 2-hydroxyisobutyrylation in developing rice (Oryza sativa) seeds. *Sci. Rep.*, **7**, 17486.
9. Fan,J., Krautkramer,K.A., Feldman,J.L. and Denu,J.M. (2015) Metabolic regulation of histone post-translational modifications. *ACS Chem. Biol.*, **10**, 95–108.
10. Huang,H., Sabari,B.R., Garcia,B.A., Allis,C.D. and Zhao,Y. (2014) SnapShot: histone modifications. *Cell*, **159**, 458–458.
11. Tcherkez,G., Boex-Fontvieille,E., Mahé,A. and Hodges,M. (2012) Respiratory carbon fluxes in leaves. *Curr. Opin. Plant Biol.*, **15**, 308–314.
12. Rylott,E.L., Rogers,C.A., Gilday,A.D., Edgell,T., Larson,T.R. and Graham,I.A. (2003) Arabidopsis mutants in short-and medium-chain acyl-CoA oxidase activities accumulate acyl-CoAs and reveal that fatty acid β-oxidation is essential for embryo development. *J. Biol. Chem.*, **278**, 21370–21377.
13. Graham,I.A. and Eastmond,P.J. (2002) Pathways of straight and branched chain fatty acid catabolism in higher plants. *Prog. Lipid Res.*, **41**, 156–181.
14. Rothbart,S.B. and Strahl,B.D. (2014) Interpreting the language of histone and DNA modifications. *Biochim. Biophys. Acta*, **1839**, 627–643.
15. Chen,X., Ding,A.B. and Zhong,X. (2020) Functions and mechanisms of plant histone deacetylases. *Sci. China Life Sci.*, **63**, 206–216.
16. Wei,W., Liu,X., Chen,J., Gao,S., Lu,L., Zhang,H., Ding,G., Wang,Z., Chen,Z. and Shi,T. (2017) Class I histone deacetylases are major histone decrotonylases: evidence for critical and broad function of histone crotonylation in transcription. *Cell Res.*, **27**, 898–915.
17. Kaczmarska,Z., Ortega,E., Goudarzi,A., Huang,H., Kim,S., Márquez,J.A., Zhao,Y., Khochbin,S. and Panne,D. (2017) Structure of p300 in complex with acyl-CoA variants. *Nat. Chem. Biol.*, **13**, 21.
18. Huang,H., Tang,S., Ji,M., Tang,Z., Shimada,M., Liu,X., Qi,S., Locasale,J.W., Roeder,R.G. and Zhao,Y. (2018) P300-mediated lysine 2-hydroxyisobutyrylation regulates glycolysis. *Mol. Cell*, **70**, 663–678.
19. Lu,Y., Xu,Q., Liu,Y., Yu,Y., Cheng,Z.-Y., Zhao,Y. and Zhou,D.-X. (2018) Dynamics and functional interplay of histone lysine butyrylation, crotonylation, and acetylation in rice under starvation and submergence. *Genome Biol.*, **19**, 144.
20. Liu,X., Wei,W., Zhu,W., Su,L., Xiong,Z., Zhou,M., Zheng,Y. and Zhou,D.X. (2017) Histone deacetylase AtSRT1 links metabolic flux and stress response in arabidopsis. *Mol Plant*, **10**, 1510–1522.
21. Zhang,F., Wang,L., Ko,E.E., Shao,K. and Qiao,H. (2018) Histone deacetylases SRT1 and SRT2 interact with ENAP1 to mediate ethylene-induced transcriptional repression. *Plant Cell*, **30**, 153–166.
22. Kim,J.-M., To,T.K., Matsui,A., Tanoi,K., Kobayashi,N.I., Matsuda,F., Habu,Y., Ogawa,D., Sakamoto,T. and Matsunaga,S. (2017) Acetate-mediated novel survival strategy against drought in plants. *Nature Plants*, **3**, 17097.
23. Kim,W., Latrasse,D., Servet,C. and Zhou,D.-X. (2013) Arabidopsis histone deacetylase HDA9 regulates flowering time through repression of AGL19. *Biochem. Biophys. Res. Commun.*, **432**, 394–398.
24. Ueda,M., Matsui,A., Tanaka,M., Nakamura,T., Abe,T., Sako,K., Sasaki,T., Kim,J.-M., Ito,A. and Nishino,N. (2017) The distinct roles of class I and II RPD3-like histone deacetylases in salinity stress response. *Plant Physiol.*, **175**, 1760–1773.
25. Liu,X., Chen,C.-Y., Wang,K.-C., Luo,M., Tai,R., Yuan,L., Zhao,M., Yang,S., Tian,G. and Cui,Y. (2013) PHYTOCHROME INTERACTING FACTOR3 associates with the histone deacetylase HDA15 in repression of chlorophyll biosynthesis and photosynthesis in etiolated Arabidopsis seedlings. *Plant Cell*, **25**, 1258–1273.
26. Li,H., Soriano,M., Cordewener,J., Muiño,J.M., Riksen,T., Fukuoka,H., Angenent,G.C. and Boutilier,K. (2014) The histone deacetylase inhibitor trichostatin a promotes totipotency in the male gametophyte. *Plant Cell*, **26**, 195–209.
27. Tian,L., Wang,J., Fong,M.P., Chen,M., Cao,H., Gelvin,S.B. and Chen,Z.J. (2003) Genetic control of developmental changes induced by disruption of Arabidopsis histone deacetylase 1 (AtHD1) expression. *Genetics*, **165**, 399–409.
28. Mair,A., Pedrotti,L., Wurzinger,B., Anrather,D., Simeunovic,A., Weiste,C., Valerio,C., Dietrich,K., Kirchler,T. and Nägele,T. (2015) SnRK1-triggered switch of bZIP63 dimerization mediates the low-energy response in plants. *Elife*, **4**, e05828.

29. Zhou,S., Liu,X., Zhou,C., Zhou,Q., Zhao,Y., Li,G. and Zhou,D.-X. (2016) Cooperation between the H3K27me3 chromatin mark and non-CG methylation in epigenetic regulation. *Plant Physiol.*, **172**, 1131–1141.
30. Chen,Q., Chen,X., Wang,Q., Zhang,F., Lou,Z., Zhang,Q. and Zhou,D.-X. (2013) Structural basis of a histone H3 lysine 4 demethylase required for stem elongation in rice. *PLoS Genet.*, **9**, e1003239.
31. Bolger,A.M., Lohse,M. and Usadel,B. (2014) Trimmomatic: a flexible trimmer for Illumina sequence data. *Bioinformatics*, **30**, 2114–2120.
32. Livak,K.J. and Schmittgen,T.D. (2001) Analysis of relative gene expression data using real-time quantitative PCR and the 2−ΔΔCT method. *Methods*, **25**, 402–408.
33. Chen,S., Zhou,Y., Chen,Y. and Gu,J. (2018) fastp: an ultra-fast all-in-one FASTQ preprocessor. *Bioinformatics*, **34**, i884–i890.
34. Kim,D., Langmead,B. and Salzberg,S.L. (2015) HISAT: a fast spliced aligner with low memory requirements. *Nat. Methods*, **12**, 357–360.
35. Liao,Y., Smyth,G.K. and Shi,W. (2014) featureCounts: an efficient general purpose program for assigning sequence reads to genomic features. *Bioinformatics*, **30**, 923–930.
36. Love,M.I., Huber,W. and Anders,S. (2014) Moderated estimation of fold change and dispersion for RNA-seq data with DESeq2. *Genome Biol.*, **15**, 550.
37. Du,Z., Zhou,X., Ling,Y., Zhang,Z. and Su,Z. (2010) agriGO: a GO analysis toolkit for the agricultural community. *Nucleic Acids Res.*, **38**, W64–W70.
38. Lu,L., Chen,X., Sanders,D., Qian,S. and Zhong,X. (2015) High-resolution mapping of H4K16 and H3K23 acetylation reveals conserved and unique distribution patterns in Arabidopsis and rice. *Epigenetics*, **10**, 1044–1053.
39. Roudier,F., Ahmed,I., Bérard,C., Sarazin,A., Mary-Huard,T., Cortijo,S., Bouyer,D., Caillieux,E., Duvernois-Berthet,E. and Al-Shikhley,L. (2011) Integrative epigenomic mapping defines four main chromatin states in Arabidopsis. *EMBO J.*, **30**, 1928–1938.
40. Jain,A. and Tuteja,G. (2019) TissueEnrich: Tissue-specific gene enrichment analysis. *Bioinformatics*, **35**, 1966–1967.
41. Trefely,S., Lovell,C.D., Snyder,N.W. and Wellen,K.E. (2020) Compartmentalized acyl-CoA metabolism and roles in chromatin regulation. *Mol. Metab.*, **38**, 100941.
42. Li,J., Terzaghi,W. and Deng,X.W. (2012) Genomic basis for light control of plant development. *Protein Cell*, **3**, 106–116.
43. Zhang,Y., Wang,C., Xu,H., Shi,X., Zhen,W., Hu,Z., Huang,J., Zheng,Y., Huang,P., Zhang,K.-X. *et al.* (2019) HY5 contributes to light-regulated root system architecture under a root-covered culture system. *Front. Plant Sci.*, **10**, 1490.
44. Zhao,S., Zhang,X. and Li,H. (2018) Beyond histone acetylation—writing and erasing histone acylations. *Curr. Opin. Struct. Biol.*, **53**, 169–177.
45. Pandey,R., MuÈller,A., Napoli,C.A., Selinger,D.A., Pikaard,C.S., Richards,E.J., Bender,J., Mount,D.W. and Jorgensen,R.A. (2002) Analysis of histone acetyltransferase and histone deacetylase families of Arabidopsis thaliana suggests functional diversification of chromatin modification among multicellular eukaryotes. *Nucleic Acids Res.*, **30**, 5036–5055.
46. Chen,X., Lu,L., Mayer,K.S., Scalf,M., Qian,S., Lomax,A., Smith,L.M. and Zhong,X. (2016) POWERDRESS interacts with HISTONE DEACETYLASE 9 to promote aging in Arabidopsis. *Elife*, **5**, e17214.
47. Sabari,B.R., Zhang,D., Allis,C.D. and Zhao,Y. (2017) Metabolic regulation of gene expression through histone acylations. *Nat. Rev. Mol. Cell Biol.*, **18**, 90–101.
48. Rousseaux,S. and Khochbin,S. (2015) Histone acylation beyond acetylation: terra incognita in chromatin biology. *Cell Journal (Yakhteh)*, **17**, 1.
49. Zhang,K., Sridhar,V.V., Zhu,J., Kapoor,A. and Zhu,J.K. (2007) Distinctive core histone post-translational modification patterns in *Arabidopsis thaliana*. *PLoS One*, **2**, e1210.
50. Bergmuller,E., Gehrig,P.M. and Gruissem,W. (2007) Characterization of post-translational modifications of histone H2B-variants isolated from Arabidopsis thaliana. *J. Proteome Res.*, **6**, 3655–3668.
51. Driscoll,R., Hudson,A. and Jackson,S.P. (2007) Yeast Rtt109 promotes genome stability by acetylating histone H3 on lysine 56. *Science*, **315**, 649–652.
52. Cote,J.M., Kuo,Y.-M., Henry,R.A., Scherman,H., Krzizike,D.D. and Andrews,A.J. (2019) Two factor authentication: Asf1 mediates crosstalk between H3 K14 and K56 acetylation. *Nucleic Acids Res.*, **47**, 7380–7391.
53. Vogt,T. (2010) Phenylpropanoid biosynthesis. *Mol. Plant*, **3**, 2–20.
54. Fraser,C.M. and Chapple,C. (2011) The phenylpropanoid pathway in Arabidopsis. *Arabidopsis Book/Am. Soc. Plant Biol.*, **9**, e0152.
55. Zeng,X., Gao,Z., Jiang,C., Yang,Y., Liu,R. and He,Y. (2020) HISTONE DEACETYLASE 9 functions with polycomb silencing to repress FLOWERING LOCUS C expression. *Plant Physiol.*, **182**, 555–565.
56. Yang,C., Shen,W., Yang,L., Sun,Y., Li,X., Lai,M., Wei,J., Wang,C., Xu,Y., Li,F. *et al.* (2020) HY5-HDA9 module transcriptionally regulates plant autophagy in response to light-to-dark conversion and nitrogen starvation. *Molecular Plant*, **13**, 515–531.
57. Yang,L., Chen,X., Wang,Z., Sun,Q., Hong,A., Zhang,A., Zhong,X. and Hua,J. (2019) HOS15 and HDA9 negatively regulate immunity through histone deacetylation of intracellular immune receptor NLR genes in Arabidopsis. *New Phytol.*, **226**, 507–522.
58. Zheng,Y., Ding,Y., Sun,X., Xie,S., Wang,D., Liu,X., Su,L., Wei,W., Pan,L. and Zhou,D.X. (2016) Histone deacetylase HDA9 negatively regulates salt and drought stress responsiveness in Arabidopsis. *J. Exp. Bot.*, **67**, 1703–1713.
59. Wang,Y., Hu,Q., Wu,Z., Wang,H., Han,S., Jin,Y., Zhou,J., Zhang,Z., Jiang,J., Shen,Y. *et al.* (2017) HISTONE DEACETYLASE 6 represses pathogen defence responses in *Arabidopsis thaliana*. *Plant Cell Environ.*, **40**, 2972–2986.
60. Hao,Y., Wang,H., Qiao,S., Leng,L. and Wang,X. (2016) Histone deacetylase HDA6 enhances brassinosteroid signaling by inhibiting the BIN2 kinase. *Proc. Natl. Acad. Sci. U.S.A.*, **113**, 10418–10423.